Natural Resonance Theory: II. Natural Bond Order and Valency

E. D. GLENDENING,* F. WEINHOLD

Theoretical Chemistry Institute and Department of Chemistry, University of Wisconsin, Madison, Wisconsin 53706

ABSTRACT: Resonance weights derived from the Natural Resonance Theory (NRT), introduced in the preceding paper are used to calculate ''natural bond order,'' ''natural atomic valency,'' and other atomic and bond indices reflecting the resonance composition of the wave function. These indices are found to give significantly better agreement with observed properties (empirical valency, bond lengths) than do corresponding MO-based indices. A characteristic feature of the NRT treatment is the description of bond polarity by a ''bond ionicity'' index (resonance-averaged NBO polarization ratio), which replaces the ''covalent-ionic resonance'' of Pauling-Wheland theory and explicity exhibits the complementary relationship of covalency and electrovalency that underlies empirical assignments of atomic valency. We present *ab initio* NRT applications to prototype saturated and unsaturated molecules (methylamine, butadiene), polar compounds (fluoromethanes), and open-shell species: (hydroxymethyl radical) to demonstrate the numerical stability, convergence, and chemical reasonableness of the NRT bond indices in comparison to other measures of valency and bond order in current usage.   © 1998 John Wiley & Sons, Inc. J Comput Chem 19: 610–627, 1998

*Present address: Department of Chemistry, Indiana State University, Terre Haute, IN 47809
    Correspondence to: F. Weinhold

    See the Editor's Note for the first paper in this series, p. 593, this issue.

Introduction

In the preceding paper, we introduced a "natural resonance theory" (NRT) formalism that allows practical calculation of effective weights $\{w_\alpha\}$ of resonance structures α for a delocalized "resonance hybrid." Unlike the Pauling-Wheland[1] treatment (based on a valence bond superposition assumption for the wave function Ψ), the NRT approach is based on the one-particle reduced density matrix $\hat{\Gamma}$,[2]

$$\hat{\Gamma} = N \int \Psi(1, 2 \ldots N) \Psi^*(1', 2 \ldots N)\, d2 \ldots dN \quad (1.1)$$

and its approximation in resonance-averaged form

$$\hat{\Gamma} \simeq \sum_\alpha w_\alpha \hat{\Gamma}_\alpha \quad (1.2a)$$

$$w_\alpha \geq 0, \qquad \sum_\alpha w_\alpha = 1 \quad (1.2b)$$

where $\hat{\Gamma}_\alpha$ is an idealized density matrix for resonance structure α. Each $\hat{\Gamma}_\alpha$ is constructed from quantities that can be obtained from natural bond orbital (NBO) analysis[3,4] using a wave function of arbitrary form, and the resonance weights w_α are chosen by a least-squares variational criterion to describe the actual $\hat{\Gamma}$ in optimal fashion. In the framework of *ab initio* molecular orbital theory, the NRT expansion (1.2) was shown to reproduce the true delocalization pattern with high accuracy (typically 80–90% or more of the delocalization density, itself a small fraction of the total electron density) for a variety of molecules and basis set levels.

Central to the resonance theory (RT) description of a delocalized molecule is the concept of *bond order* b_{AB} ("weighted average" number of bonds between A and B), which can be correlated with empirical bond length, bond energy, and other properties.[5] In its most basic form. the formal bond order between atoms A and B is defined as[6]

$$b_{AB} = \sum_\alpha w_\alpha b_{AB}^{(\alpha)} \quad (1.3)$$

where $b_{AB}^{(\alpha)}$ is the (integer) number of bonds in the idealized Lewis-type structural formula for resonance structure α. In accordance with the intermediate character of the resonance hybrid, bond properties corresponding to fractional b_{AB} are expected to be intermediate between those for idealized integer bond orders of completely localized structures.

A prototype example of resonance mixing is furnished by the formamide molecule (NH_2CHO), which is expected to be primarily described by the parent resonance structure (I), with strong admixture of the charge-separated structure (II),
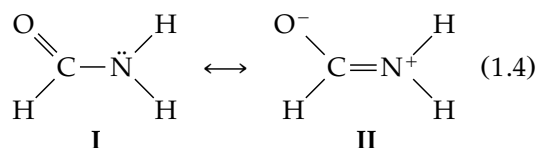
and lesser contributions from other resonance structures. From empirical considerations, Pauling[7] estimated the relative contributions of structures I and II to be about 60% and 40%, respectively, leading to formal bond orders

$$b_{CO} = (0.60)(2) + (0.40)(1) = 1.60$$
$$b_{CN} = (0.60)(1) + (0.40)(2) = 1.40 \quad (1.5)$$

corresponding to significant C=N double bond character. [For comparison, NRT analysis of an *ab initio* MP2/6-31G* wave function for formamide (optimized C_s geometry) gives leading weights $w_I = 59.29\%$ and $w_{II} = 27.87\%$ and bond orders $b_{CO} = 1.7277$ and $b_{CN} = 1.3289$, in crude agreement with Pauling's analysis.] As is well known,[8] Pauling's recognition of this partial b_{CN} double-bond character (leading to planar peptide groups) played an important role in the discovery of the α-helix in proteins. Pauling's monograph[1(b)] presents many other illustrations of how RT and bond order concepts can be used to rationalize molecular properties in a simple, chemically intuitive manner.

A principal aim of the present paper is to present *ab initio* NRT weightings and bond indices for prototypical cases of resonance mixing, in order to test their consistency with general RT concepts, determine their general numerical characteristics (stability and convergence with respect to changes in level of theory, NRT program parameters, etc.), and establish the degree of correlation with empirical valency and geometrical parameters. As was pointed out in the preceding paper, Pauling-Wheland RT encountered formal and practical difficulties which effectively led to its demise for quantitative *ab initio* purposes, and formulas such as (1.3) were eventually replaced by MO-based measures of bond order in which "resonance struc-

tures'' and ''resonance weights'' play no direct role. Full assessment of the NRT method therefore involves comparisons with alternative MO-based bond indices that are widely employed in current *ab initio* and semiempirical studies.

The plan of the paper is as follows: We describe the NRT formulation of bond order and atomic valency in the next section, showing how it differs from Pauling-Wheland bond order in the treatment of ''covalent-ionic resonance.'' Next, alternative MO-based measures of bond order and valency are reviewed. Thereafter, selected NRT applications are presented to ''ordinary'' saturated (methylamine), unsaturated (butadiene), polar covalent (fluoromethanes), and open-shell species (hydroxymethyl radical) to illustrate characteristic numerical features of the method in typical cases of weak or moderate delocalization. (Cases of extreme delocalization or ''anomalous'' bonding are described in the following paper.) The final section presents a summary and conclusions.

Bond Order and Atomic Valency: NRT Definitions

Given the natural resonance weights $w_\alpha^{(N)}$, as determined from the NRT variational function (preceding paper), one obtains the ''natural bond order'' $b_{AB}^{(N)}$ by direct analogy with the classical expression (1.1),

$$b_{AB}^{(N)} = \sum_\alpha^{n_{RS}} w_\alpha^{(N)} b_{AB}^{(\alpha)} \tag{2.1}$$

where $b_{AB}^{(\alpha)}$ is the *integer* $(0, 1, 2\ldots)$ number of A—B bonds in the structural formula for the αth natural Lewis structure. Because alternative MO-based methods (see next section) generally do not involve explicit prediction of resonance weights w_α, the comparison of NRT results to these methods must be carried out directly in terms of bond order values, as will be numerically illustrated below for several prototype molecules.

Closely related to formal bond order is the notion of atomic valency[9] V_A of atom A. This can be regarded as a measure of total bond-making capacity exhibited by atom A in the molecule, obtained by summing the formal bond orders over all possible atoms B. Accordingly, we define the ''natural atomic valency'' $V_A^{(N)}$ as

$$V_A^{(N)} = {\sum_B}' b_{AB}^{(N)} \tag{2.2}$$

where the prime denotes omission of the term A = B. Qualitatively speaking, the valencies $V_A^{(N)}$ for elements of groups IV–VII are expected to match the respective empirical values 4, 3, 2, 1 (8 − group number) in all but exceptional (hypervalent, hypovalent) cases.

The definitions (2.1) and (2.2) [in conjunction with the positivity property (1.2b)] intrinsically prevent the appearance of *negative* bond order or atomic valency in the NRT formalism.[10]

$$b_{AB}^{(N)} \geq 0, \; V_A^{(N)} \geq 0, \; \text{all A, B} \tag{2.3}$$

The limiting values $b_{AB}^{(N)} = 0$ and $V_A^{(N)} = 0$ are attained in the limit of vanishing bonding interactions (e.g., two He atoms at infinite separation). Weak ''nonbonded interactions'' between atoms in different molecular units are reflected in small bond orders $(0 < b_{AB}^{(N)} \ll 1)$ between formally nonbonded atoms. Whereas the quantities (2.1) and (2.2) are expected to exhibit near-integer values in ordinary compounds, these formulas are intrinsically free to represent smoothly the transition between distinct limiting bond patterns.

As was remarked in the preceding paper, our formulation differs markedly from that of Pauling-Wheland RT (and related MO-based) methods in its treatment of covalent-ionic resonance and bond ionicity. However, given the total NRT bond order (or ''coordination number'') $b_{AB}^{(N)}$ between two atoms, one can readily define the *fractional ionic character* i_{AB} as the resonance-weighted average

$$i_{AB} = \frac{\sum_\alpha w_\alpha i_{AB}^{(\alpha)}}{b_{AB}} \tag{2.4}$$

where $i_{AB}^{(\alpha)}$ is the corresponding fractional ionic character in resonance structure $\Psi_\alpha^{(L)}$, defined from the NBO polarization coefficients c_A and c_B [cf. Eq. (2.9) in the preceding paper] as

$$i_{AB}^{(\alpha)} = \left| \frac{c_A^2 - c_B^2}{c_A^2 + c_B^2} \right| \tag{2.5}$$

(averaged, if necessary, over multiple bonds). In terms of the fractional ionic character, one can formally partition the total bond order $b_{AB}^{(N)}$ into its ''electrovalent'' (ionic) and ''covalent'' contributions, $e_{AB}^{(N)}$ and $c_{AB}^{(N)}$, respectively:

$$e_{AB}^{(N)} = b_{AB}^{(N)} i_{AB} \tag{2.6}$$

$$c_{AB}^{(N)} = b_{AB}^{(N)} (1 - i_{AB}) \tag{2.7}$$

so that

$$b_{AB}^{(N)} = e_{AB}^{(N)} + c_{AB}^{(N)}. \qquad (2.8)$$

Insofar as the NRT covalent bond order $c_{AB}^{(N)}$ diminishes as the ionic character of the bond increases, this quantity should be most directly comparable to the Pauling-Wheland bond order $b_{AB}^{(PW)}$,

$$b_{AB}^{(PW)} \simeq c_{AB}^{(N)}, \qquad (2.9)$$

which is considered to vanish in the ionic limit.

By analogy with (2.2), one can also formally sum the NRT electrovalent and covalent bond orders $e_B^{(N)}$ and $c_{AB}^{(N)}$ over all bonded atoms B (whether in ionic, dative, or covalent sense) to give the total *electrovalency* $E_A^{(N)}$ and *covalency* $C_A^{(N)}$ of atom A.[9]

$$E_A^{(N)} = \sum_B{}' e_{AB}^{(N)} \qquad (2.10)$$

$$C_A^{(N)} = \sum_B{}' c_{AB}^{(N)} \qquad (2.11)$$

As is shown by (2.2) and (2.8), the *full valency* $V_A^{(N)}$ is just the sum of its electrovalent (ionic, "unshared") and covalent ("shared") contributions,

$$V_A^{(N)} = E_A^{(N)} + C_A^{(N)}. \qquad (2.12)$$

For cases of low ionic character ($i_{AB} \ll 1$), the full valency $V_A^{(N)}$ and covalency $C_A^{(N)}$ will approximately coincide, but, in more ionic cases, only the latter quantity corresponds to "valency" $V_A^{(PW)}$ in the Pauling-Wheland (or related MO-based) sense,

$$V_A^{(PW)} \simeq C_A^{(N)} \qquad (2.13)$$

The distinction drawn in (2.10)–(2.12) between the NRT definitions of electrovalency, covalency, and full valency (and the associated bond orders) have important consequences for comparisons with empirical properties. It is generally expected that reduced bond order should be associated with bond *weakening* (i.e., with increase of bond length, reduction of bond energy, red-shifting of vibrational frequencies, etc.).[5] However, *covalent* bond order $c_{AB}^{(N)}$, as defined in (2.7), can exhibit the *opposite* trend in variations that hold the total $b_{AB}^{(N)}$ constant, because it is known that a bond of higher ionic character (and, thus, of lower $c_{AB}^{(N)}$) is often strengthened with respect to analogous apolar bonds involving the same atoms[11] (a trend reflected in the characteristically high enthalpies of formation and high melting and boiling points of ionic compounds). Thus, an attempt to correlate bond lengths with $c_{AB}^{(N)}$ alone may lead to inconsis-

tencies (the bond length sometimes increasing and sometimes decreasing with $c_{AB}^{(N)}$ or with the closely related $b_{AB}^{(PW)}$), whereas the *full* NRT bond order $b_{AB}^{(N)}$ should exhibit a more consistent correlation with empirical bond properties as ionic character varies. Similarly, neither the electrovalency $E_A^{(N)}$ nor covalency $C_A^{(N)}$ can be expected to match the empirical valency $V_A^{(emp)}$, except in extreme ionic or covalent limits, whereas the *full* NRT valency $V_A^{(N)}$ should generally be in good agreement with $V_A^{(emp)}$ in compounds of widely varying ionic character. Whereas the partial bond orders ($e_{AB}^{(N)}$, $c_{AB}^{(N)}$) and valencies ($E_A^{(N)}$, $C_A^{(N)}$) are introduced for comparison with Pauling-Wheland (and related MO-based) values, only the *full* $b_{AB}^{(N)}$, $V_A^{(N)}$ are expected to exhibit satisfactory correlations with empirical properties over a wide range of ionicity.

Alternative Measures of Bond Order

The difficulties of evaluating Pauling-Wheland resonance weights and bond orders by practical quantum-chemical means have led to suggestions for alternative "bond order"-like quantities, particularly in the MO framework. These bond indices are routinely provided by popular electronic structure programs and have largely supplanted the older RT values for quantitative purposes.

In the framework of simple minimal-basis pi MO theory, Coulson[12] originally suggested that a measure of bond order is given by

$$P_{AB} = 2 \sum_i^{occ} c_{iA} c_{iB} \qquad (3.1)$$

where c_{iA} is the coefficient of AO χ_A (on atom A) in the ith occupied molecular orbital ϕ_i

$$\phi_i = \sum_A c_{iA} \chi_A. \qquad (3.2)$$

In an orthonormal basis, the right side of (3.1) is an off-diagonal element $(\underline{\Gamma})_{AB} = \langle \chi_A | \hat{\Gamma} | \chi_B \rangle$ of the one-particle density matrix between AOs χ_A and χ_B, equivalent in this case to the Fock-Dirac density matrix $\underline{P}$ ("bond-order matrix"); in the more general case, these matrices are related by

$$\underline{\underline{\Gamma}} = \underline{\underline{SPS}} \qquad (3.3)$$

where $\underline{S}$ is the AO overlap matrix. More generally, the LCAO-MO expansion (3.2) includes multiple AOs $\{\chi_r\}$ on each center, and the analogous partial bond order P_{rs} must be summed over AOs on each

atom to give the total A—B bond order $b_{AB}^{(MO)}$,

$$b_{AB}^{(MO)} = \sum_{r}^{\text{on A}} \sum_{s}^{\text{on B}} P_{rs}. \qquad (3.4)$$

We refer to (3.4) as the "MO bond order" to distinguish it from the RT-based quantity (1.1).

Although the MO bond order (3.4) achieves the expected classical values (e.g., $b_{AB}^{(MO)} = 2$ for ethylene) in limiting cases, it differs significantly from the RT value in other instances. In benzene, for example, elementary MO theory leads to $b_{CC}^{(MO)} = 1\frac{2}{3}$ for each CC bond,[12] which can no longer be easily related to a weighted average of plausible resonance structures. Moreover, the summed bond orders lead to "atomic valency" values

$$V_A^{(MO)} = \sum_{B}' b_{AB}^{(MO)} \qquad (3.5)$$

that deviate markedly from the expected integer values (e.g., $V_C^{(MO)} = 4\frac{1}{3}$ for each C atom of benzene). A further difference is that the total $b_{AB}^{(MO)}$ (or the individual orbital contributions P_{rs}) may assume *negative* values, whereas (1.1) is intrinsically positive.

Wilberg[13] originally introduced an alternative bond index

$$b_{AB}^{(W)} = \sum_{r}^{\text{on A}} \sum_{s}^{\text{on B}} P_{rs}^2 \qquad (3.6)$$

as a sum of *squared* density matrix elements. The "Wiberg bond index" $b_{AB}^{(W)}$ is intrinsically positive and is often in better agreement with classical RT values. The Wiberg bond index has been revived in many guises,[14] sometimes with confusing or conflicting terminology.[15] Wiberg originally proposed the definition (3.6) in the framework of semiempirical MO theory, where the AO basis is implicity orthonormal $[(\underline{S})_{rs} = \delta_{rs}]$, but in a nonorthogonal basis one might modify this formula by inserting various factors of overlap[16] or orthogonalizing the AOs in various ways.[17] A particularly straightforward *ab initio* implementation of the Wiberg formula involves use of natural atomic orbitals (NAOs), an orthonormal set whose properties have been shown to resemble closely those assumed in semiempirical MO treatments.[18] Such a "Wiberg NAO bond index" is routinely calculated in the general NBO program as a general guide to bond order, so we employ this specific form of the Wiberg bond index in the numerical comparisons in the following section. As an example of related nonorthogonal AO-based bond

indices, we employ the "Mayer-Mulliken bond order"[16] in which $\underline{P}$ is replaced by $\underline{\underline{PS}}$ in the Wiberg formula.

Reed and Schleyer[19] introduced a novel measure of bond order based on the form of natural localized molecular orbitals (NLMOs) in the NAO basis. The Reed-Schleyer bond order $b_{AB}^{(RS)}$ (denoted "NPA/NLMO) bond order by Reed and Schleyer[19]) is the sum over occupied NLMOs

$$b_{AB}^{(RS)} = \sum_{i}^{\text{LMOs}} b_{iAB} \qquad (3.7a)$$

of partial bond orders b_{iAB} defined as

$$b_{iAB} = \min(n_{iA}, n_{iB}) \cdot \text{sgn}(S_{iAB}) \qquad (3.7b)$$

where n_{iA} is the number of electrons on atom A in NLMO i (based on the squared LC-NAO coefficients c_{ij} in the NLMO),

$$n_{iA} = \sum_{j}^{\text{on A}} c_{ij}^2 \qquad (3.7c)$$

and $\text{sgn}(S_{iAB}) = \pm 1$ is a sign factor related to the overlap pattern. As (3.7b) indicates, $b_{AB}^{(RS)}$ acquires contributions only from *shared* occupancy on A and B (the lesser of n_{iA} and n_{iB}) and should thus be most directly comparable to the covalent bond order $c_{AB}^{(N)}$, eq. (2.7),

$$b_{AB}^{(RS)} \simeq c_{AB}^{(N)}. \qquad (3.8)$$

More recently, Cioslowski and Mixon[20] (CM) introduced a definition of "covalent bond order" in the framework of Bader's density partitioning method.[21] The CM bond order $b_{AB}^{(CM)}$ is based on a Wiberg-like formula using integrated electron densities from atomic "basins" defined by Bader's zero-flux criterion. The novel feature of the CM bond order is its relation to a configuration space (rather than Hilbert space or orbital) description of atoms. Some values of $b_{AB}^{(CM)}$ for C—F bonds of fluoromethanes were recently obtained by Wiberg and Rablen,[22] and will be compared to NRT and MO-based indices below.

Brown and coworkers[23] introduced a related "bond valence," which is primarily an empirical index (essentially, a way of reexpressing empirical bond length to predict atomic valencies for ionic species) and is not considered further here. Still another group of bond order formulas are based on permutation-algebraic or graph-theoretic methods.[24] These formulas are primarily topological in

nature, are restricted to idealized planar networks, and therefore do not take account of geometry variations, polarity differences, and other molecular details. Because these methods are not easily related to *ab initio* quantities, we do not consider them further in this paper.

Illustrative Numerical Applications

SATURATED MOLECULES: METHYLAMINE

We first illustrate the NRT algorithm for a simple saturated molecule, methylamine (CH_3NH_2), with the atom numbering shown below.

$$(4.1)$$
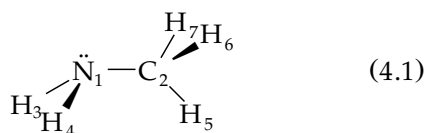
This case of weak resonance delocalization will serve to demonstrate the ability of NRT analysis to describe quantitatively subtle details of delocalization beyond the usual qualitative RT framework.

To compare weights and bond orders for different theoretical levels, we fix the molecule in idealized Pople-Gordon (PG) geometry,[25] with equal bond lengths R_{NH} (1.01 Å) and R_{CH} (1.09 Å), and tetrahedral valence angles. Table I shows the leading NRT weights for three distinct basis levels of uncorrelated MO theory [HF/3-21G (split valence double zeta), HF/6-31G* (double zeta plus polarization) and HF/6-311++G** (triple zeta with extended diffuse and polarization sets on all atoms)] and two levels of correlation treatment [MP2 (second-order Møller-Plesset theory), QCISD (quadratic configuration interaction with single and double excitations), both at 6-31G* basis level].[26] As Table I illustrates the leading delocal-

TABLE I.
NRT Resonance Weights w_i for Methylamine at Several Levels of *Ab Initio* Uncorrelated (MO) and Correlated (corr) Theory, All at Idealized Pople-Gordon Geometry.

		NRT resonance weights w_α (%)				
i	Structure	MO-1[a]	MO-2[b]	MO-3[c]	corr-1[d]	corr-2[e]
1.		97.88	97.67	97.45	92.48	91.00
2.		0.80	0.83	0.89	1.95	2.21
3.	(2)	0.26	0.31	0.33	1.31	1.65
4.	(2)	0.26	0.31	0.31	1.29	1.60
5.	(2)	0.14	0.12	0.19	0.18	0.14

[a] HF/3-21G.
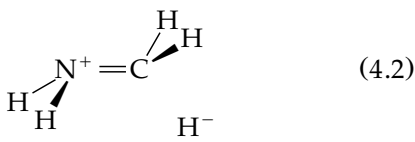[b] HF/6-31G*.
[c] HF/6-311++G**.
[d] MP2/6-31G*.
[e] QCISD/6-31G*.

ization correction arises from the "double bond–no bond" resonance structure

$$H\underset{H}{\overset{H}{\diagdown}}N^{+}=C\underset{H}{\overset{H}{\diagup}}\underset{H^{-}}{\overset{H}{\diagdown}} \tag{4.2}$$

associated with the $n_N \rightarrow \sigma^*_{CH_5}$ NBO interaction of the nitrogen lone pair with the antiperiplanar σ^*_{CH} antibond. It can be seen that the three MO results agree closely, showing the excellent stability and convergence of the NRT method with respect to basis expansion. The two correlated treatments give appreciably higher resonance delocalization (about 1% higher for each of the three most important delocalization structures), and this tendency of electron correlation to enhance delocalization seems to be a rather general effect. There is good overall agreement in the pattern of relative weightings in correlated and uncorrelated treatments (e.g., structure 2 is weighted about 0.6% above structure 3 in both treatments), demonstrating that qualitative aspects of resonance delocalization are already present at the uncorrelated MO level, with electron correlation providing quantitative enhancement, rather than qualitatively new types, of resonance delocalization.

Table II shows the corresponding results for the NRT bond orders and atomic valencies, comparing these with the RHF/6-31G* values of the Wiberg (WBI), Mayer-Mulliken (MM), and Reed-Schleyer (RS) bond indices. [The MM values would show considerable variations in higher basis sets,[16] but the (NAO-based) WBI and RS values are stable, so the RHF/6-31G* values may be taken as representative of other basis levels.] The agreement among the various NRT quantities is excellent, with a perceptibly enhanced CN bond order (ca. 1.08 vs. 1.02) and slightly diminished CH and NH bond orders (0.97 vs. 0.99) at correlated levels. The MO-based indices (which should only be compared to uncorrelated NRT indices) show rather less orderly patterns. The NRT atomic valences are seen to be in consistent, excellent agreement with the expected empirical valency (viz. 4.00 for C, 3.01 ± 0.01 for N, 0.98 ± 0.01 for H), whereas the deviations of WBI, MM, and RS valencies from expected empirical values are much greater (often by an order of magnitude or more). Note that the NRT hydrogen valency V_H essentially coincides (except in cases such as H-bonding or bridge-bonding: see the following paper) with its formal bond order to the directly bonded atom, whereas the WBI, MM, and RS valencies have numerous small contribu-

TABLE II.

Natural Bond Orders and Atomic Valencies of Methylamine (Corresponding to the Entries in Table I), with Comparison WBI, MM, and RS Bond Indices (RHF / 6-31G*) (see (4.1) for Atom Numbering).

A—B bond	NRT bond order b_{AB}					Other b_{AB}		
	MO-1[a]	MO-2[b]	MO-3[c]	corr-1[d]	corr-2[e]	WBI[b]	MM[b]	RS[b]
C—N	1.0212	1.0233	1.0255	1.0752	1.0900	1.0056	0.9341	0.8209
N—H$_4$	0.9948	0.9932	0.9936	0.9740	0.9675	0.8502	0.8581	0.6208
C—H$_5$	0.9920	0.9918	0.9911	0.9805	0.9779	0.9494	0.9595	0.8039
C—H$_6$	0.9934	0.9925	0.9917	0.9722	0.9661	0.9430	0.9602	0.7844

Atom	NRT atomic valency V_A					Other V_A		
	MO-1[a]	MO-2[b]	MO-3[c]	corr-1[d]	corr-2[e]	WBI[b]	MM[b]	RS[b]
C	4.0000	4.0000	4.0000	4.0000	4.0000	3.8465	3.7996	3.1919
N	3.0109	3.0108	3.0127	3.0232	3.0249	2.7383	2.6174	2.0362
H$_4$	0.9948	3.0109	0.9948	0.9740	0.9645	0.8636	0.8482	0.6272
H$_5$	0.9920	0.9918	0.9911	0.9805	0.9779	0.9716	0.9273	0.7891
H$_6$	0.9934	0.9925	0.9917	0.9722	0.9661	0.9593	0.9310	0.7844

[a] HF / 3-21G.
[b] HF / 6-31G*.
[c] HF / 6-311++ G**.
[d] MP2 / 6-31G*.
[e] QCISD / 6-31G*.

tions from nonbonded atoms that appreciably alter the ''expected'' value.

Also, from the fully optimized bond lengths (e.g., CN = 1.4533 Å, NH_4 = 1.0015 Å, CH_5 = 1.0908 Å, CH_6 = 1.0838 Å at the RHF/6-31G* level), one can recognize that the NRT bond orders are in improved correlation with structural features.[27] For example, at all uncorrelated MO levels, the NRT bond orders are slightly *larger* for CH_6 than for CH_5, consistent with the observed slight increased in optimized CH_5 bond length, whereas the WBI and RS indices predict the opposite trend. Further examples will be cited below to demonstrate the improved order-bond length correlations (which are not globally linear; cf. Fig 4 in the following paper) to be an important advantage of the NRT quantities.

However, Table II also shows the somewhat disturbing result that the bond orders are smaller for CH_6 than for CH_5 at the correlated levels, despite the greater CH_5 bond length at all levels (consistent with the leading $n_H \to \sigma^*_{CH_5}$ delocalization that gives rise to structure 2 in Table I). This points to a characteristic difficulty of the NRT bond order-bond length correlations. Formally, the $\sigma_{AB} \to \sigma^*_{CD}$ NBO delocalization leads to an equal decrease in A—B and C—D bond orders and a simultaneous equal increase in B—C bond order [cf. mnemonic (4.3) in the preceding paper]. However, there is no physical reason why such delocalization should produce identical $|\Delta R_{AB}|$, $|\Delta R_{BC}|$, and $|\Delta R_{CD}|$ bond length changes. Indeed, experience has shown that *removal* of a small amount of electron density from a filled donor NBO σ_{AB} seems to have a significantly *weaker* effect on bond length than addition of the equivalent amount of electron density to an unfilled acceptor NBO σ^*_{CD},

and neither ΔR_{AB} nor ΔR_{CD} is likely to be equal in magnitude to the change in the connecting bond R_{BC} as the $\sigma_{AB} \to \sigma^*_{CD}$ interaction ''turns on.'' Thus, the delocalization corresponding to structure 3 in Table I is likely to have significantly less effect on C—H bond length than that of structure 4 (whereas 3 has greater effect than 4 on N—H bond length), even though the formal bond order changes are identical. As is shown in Table I, at uncorrelated levels the weights of structures 3 and 4 are sufficiently small compared to the leading delocalization 2 that no anomalies are evident ($w_3 + w_4 < w_2$), whereas at correlated levels the relative roles are reversed. Subtle anomalies of this type are expected to affect the details and limit the accuracy of bond order-bond length correlations that crudely assume equal bond length changes for equal changes in formal bond order (regardless of physical origin). Nevertheless, as the numerical examples below will show, these subtleties do not appear to detract seriously from the qualitative validity of conventional bond order-bond length correlations.

It is also important to understand the dependence of individual resonance weights and bond orders on NRT program parameters, particularly the NRT energetic threshold NRTTHR that controls the magnitude of delocalization effects to be investigated (and thus the number of resonance structures n_{RS} considered). Table III presents the results of such threshold variations at the RHF/6-31G* level, showing the change in resonance weights w_i as NRTTHR is systematically raised from its default value (1.0 kcal/mol) by 0.5 kcal/mol increments. Table III illustrates a remarkable property of the NRT expansion [cf. eq. (4.15) in the preceding paper], namely, that the

TABLE III.
Variations of n_{RS} (Number of Resonance Structures) and NRT Weightings w_i with Changes in NRTTHR Energetic Threshold for Methylamine (RHF / 6-31G* Level).

NRTTHR (kcal / mol)	n_{RS}	NRT resonance weights (%)				
		w_1	w_2	w_3	w_4	w_5
1.0	8	97.67	0.89	0.31	0.31	0.12
1.5	6	97.68	0.95	0.31	0.38	—
2.0	6	97.68	0.95	0.31	0.38	—
2.5	6	97.68	0.95	0.31	0.38	—
3.0	6	97.68	0.95	0.31	0.38	—
3.5	4	98.43	0.95	0.31	—	—
4.0	2	99.05	0.95	—	—	—
...	2	99.05	0.95	—	—	—
9.0	1	100.00	—	—	—	—

percentage weights of secondary structures are often *practically independent of other resonance structures included in the expansion* (each w_i being dictated primarily by its associated stabilization energy ΔE_i). As was remarked in the preceding paper this behavior is expected when a resonance structure involves an acceptor NBO that is not shared with other resonance structures of comparable weighting (i.e., if two delocalizations are not "cooperatively coupled"). A rough rule of thumb is that the resonance weight w_i (in percentage units) of a secondary structure is approximately an order of magnitude smaller than the associated ΔE_i (in kcal/mol). The entries in Table II serve to illustrate this rough proportionality. This example suggests that one can rather freely adjust the NRT-THR threshold to suppress less important delocalization (and speed execution) without appreciably altering the relative weights of the structures retained.

Finally, we examine the "discontinuity" in weighting that may occur when a resonance structure is arbitrarily treated as a reference (rather than secondary) structure.[28] Table IV shows NRT weightings for methylamine (RHF/6-31G* level) when additional structures are successively specified as reference structures with the $NRTSTR keylist (though structures 3 and 4 were ultimately rejected as reference structures in this example). In the present example, each secondary w_i is apparently boosted by about 0.6% when promoted to reference structure status. This "jump" emphasizes that the NRT weightings have relative rather than absolute significance and that valid comparisons of two systems should be based on a consistent choice of reference structures.
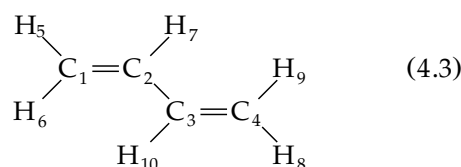
TABLE IV.
Variations of NRT Weightings w_i for Methylamine (RHF/6-31G* Level) with Respect to Choice of Reference Structures (Specified by $NRTSTR Keylist; Only Bracketed Entries Were Accepted as Final Reference Structures).

Reference structures	NRT resonance weights (%)				
	w_1	w_2	w_3	w_4	w_5
1	[97.67]	0.83	0.31	0.31	0.12
1, 2	[96.98]	[1.47]	0.30	0.31	0.12
1–4	[96.98]	[1.47]	0.30	0.31	0.12
1–5	[95.91]	[1.48]	0.29	0.29	[0.71]

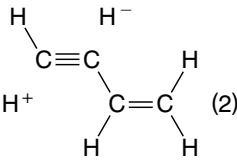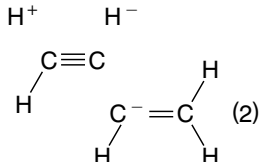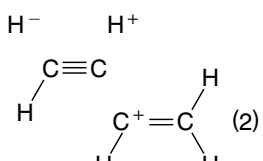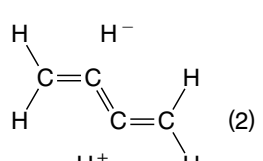## UNSATURATED MOLECULES: BUTADIENE AND ISOMERS
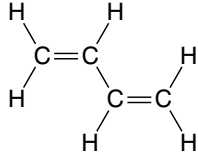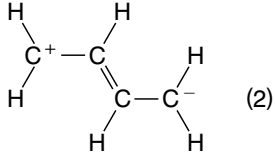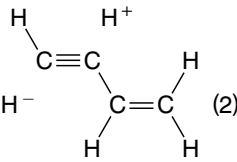
As a typical unsaturated molecule, we consider the example of 1,3-butadiene. For the *trans* conformation, with idealized PG geometry (CC = 1.34 Å, CH = 1.08 Å, trigonal valence angles), we apply the same five *ab initio* methods considered above, leading to the NRT weightings shown in Table V.[29] The principal delocalization correction is the dipolar structure (entry 2 in Table V) that can be crudely associated with the conventional "long-bond"[30] covalent structure of Pauling-Wheland theory. As expected, weights of the leading resonance correlations are significantly higher than in the saturated methylamine case, reflecting the stronger diene conjugative delocalization. Most striking in Table V is the evident effectiveness of electron correlation in enhancing resonance delocalization (e.g., increasing the weight of the leading resonance correction from about 2.8% to 6.9%). However, as in the saturated case, electron correlation enhances a pattern that is already present in the uncorrelated MO treatment, rather than introducing qualitatively new resonance structures.

For this conjugated system, Table V verifies the excellent NRT numerical characteristics that were previously noted in the saturated case, including the practical invariance to choice of basis set. Table VI displays the corresponding butadiene NRT bond orders (for idealized PG geometry) at each level, with the atom numbering shown below.

$$\begin{array}{c} H_5 \qquad\qquad H_7 \\ \diagdown\qquad\qquad\diagup \\ C_1 = C_2 \qquad\qquad H_9 \\ \diagup\qquad\qquad\qquad\diagup \\ H_6 \qquad\qquad C_3 = C_4 \\ \diagup\qquad\qquad\diagdown \\ H_{10}\qquad\qquad H_8 \end{array} \qquad (4.3)$$

Very satisfactory numerical stability is evident in these results (e.g., bond orders for all three MO levels typically agree within a few parts per thousand) as well as good overall agreement in bond order patterns for correlated and uncorrelated wave functions. Table VI also includes corresponding WBI, MM, and RS bond indices (RHF/6-31G* level) for comparison as well as the fully optimized (RHF/6-31G* level) bond lengths, R_{CC} and R_{CH}, in the final column. Comparison of the NRT bond orders with optimized bond lengths shows the good correlation (even to small details of CH bond length; see below). In this case the WBI, MM, and RS values show qualitatively similar bond order patterns (though the WBI and MM values incorrectly suggest very similar values of CH_5,

TABLE V.

Leading NRT Resonance Weights w_i for *trans*-Butadiene at Several Levels of *Ab Initio* Uncorrelated (MO) and Correlated (corr) Theory (Idealized PG Geometry).

i	Structure	NRT resonance weights (%)				
		MO-1[a]	MO-2[b]	MO-3[c]	corr-1[d]	corr-2[e]
1.		89.79	89.96	89.27	74.47	70.96
2.	(2)	2.65	2.56	2.83	6.93	7.92
3.	(2)	0.41	0.40	0.49	1.49	1.75
4.	(2)	0.36	0.35	0.44	1.42	1.78
5.	(2)	0.33	0.34	0.41	1.12	1.37
6.	(2)	0.30	0.32	0.35	1.18	1.32
7.	(2)	0.17	0.28	0.34	0.00	0.27

[a] HF / 3-21G.
[b] HF / 6-31G*.
[c] HF / 6-311 + + G**.
[d] MP2 / 6-31G*.
[e] QCISD / 6-31G*.

TABLE VI.
Natural Bond Orders and Atomic Valencies of _trans_-Butadiene (Corresponding to the Entries in Table V), With Comparison WBI, MM, and RS Bond Indices (RHF / 6-31G*) (see (4.3) for Atom Numbering).

A—B bond	NRT bond order b_{AB}					Other b_{AB}			$R_{AB}^{\text{opt b}}$ Å
	MO-1[a]	MO-2[b]	MO-3[c]	corr-1[d]	corr-2[e]	WBI[b]	MM[b]	RS[b]	
C_1—C_2	1.9524	1.9552	1.9553	1.9133	1.9027	1.9200	1.8901	1.9294	1.3227
C_2—C_3	1.0378	1.0392	1.0451	1.0941	1.1099	1.0867	1.0762	1.0533	1.4676
C_1—H_5	0.9924	0.9921	0.9912	0.9744	0.9731	0.9406	0.9557	0.7823	1.0748
C_1—H_6	0.9911	0.9907	0.9899	0.9709	0.9647	0.9405	0.9555	0.7876	1.0766
C_2—H_7	0.9853	0.9845	0.9824	0.9639	0.9582	0.9204	0.9446	0.7619	1.0782

[a] HF / 3-21G.
[b] HF / 6-31G*.
[c] HF / 6-311++ G**.
[d] MP2 / 6-31G*.
[e] QCISD / 6-31G*.

and CH_6 compared to CH_7). The WBI, MM, and RS atomic valencies (not shown) again deviate much more from expected empirical values than do the NRT quantities.

To exhibit the variations of calculated bond order with geometrical changes, we carried out a rigid torsional rotation about the C_2—C_3 axis (dihedral angle ϕ) to convert the _trans_ to the _cis_ isomer (holding all other variables fixed in idealized PG form). Figure 1 shows the calculated variations of NRT b_{CC} and b_{CH} "single" bond orders through this transition. (Bond orders for fully opti-
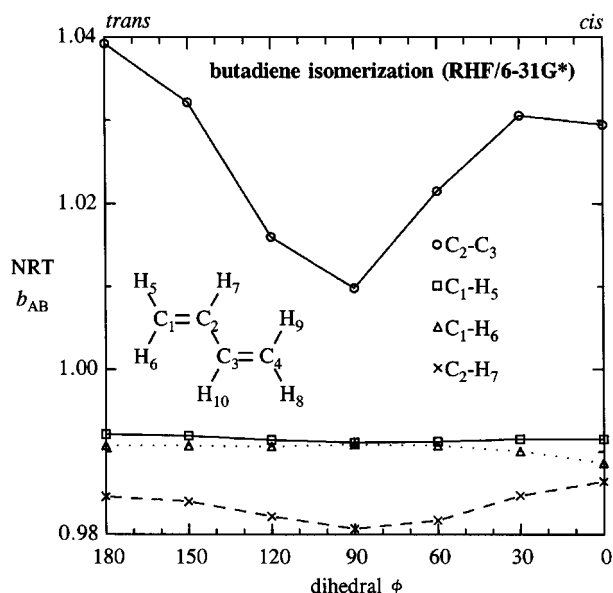

FIGURE 1. Variations of NRT bond orders b_{CC} and b_{CH} with dihedral angle ϕ in butadiene _trans–cis_ isomerization (RHF / 6-31G* level, rigid-rotor Pople-Gordon geometry).

mized geometries are very similar, accentuating the subtle variations that are already exhibited in idealized PG geometry.) The central $b_{C_2C_3}$ bond order varies most strongly, dropping (from $b_{C_2C_3}$ = 1.0392) to nearly pure single bond character ($b_{C_2C_3}$ = 1.0098) as the pi bonds are twisted out of conjugation to ϕ = 90°, then rising again (to $b_{C_2C_3}$ = 1.0295) in the planar _cis_ arrangement, in good agreement with the expected chemical behavior. Figure 2a displays the correlation of calculated CC bond order (idealized geometry) with "relaxed" CC bond lengths (fully optimized RHF/6-31G* level) for both types of CC bonds, showing that the bond lengths change in response to bond order differences in the expected manner. However, as Figure 1 shows, the CH bond orders (especially $b_{C_2H_7}$) undergo still more subtle variations that can also be qualitatively correlated with actual bond length changes. For example, Figure 1 suggests that at the twisted 90° conformation, C_1—H_5 and C_1—H_6 should be nearly identical, and significantly shorter than C_2—H_7, whereas, at the 0° _cis_ arrangement, the three bond lengths should be more nearly comparable, with C_1—H_6 intermediate between C_1—H_5 and C_2—H_7. The fully optimized bond lengths

90° : C_1—H_5 = 1.0758 Å, C_1—H_6 = 1.0761 Å,

C_2—H_7 = 1.0793 Å

0° : C_1—H_5 = 1.0748 Å, C_1—H_6 = 1.0755 Å,

C_2—H_7 = 1.0777 Å

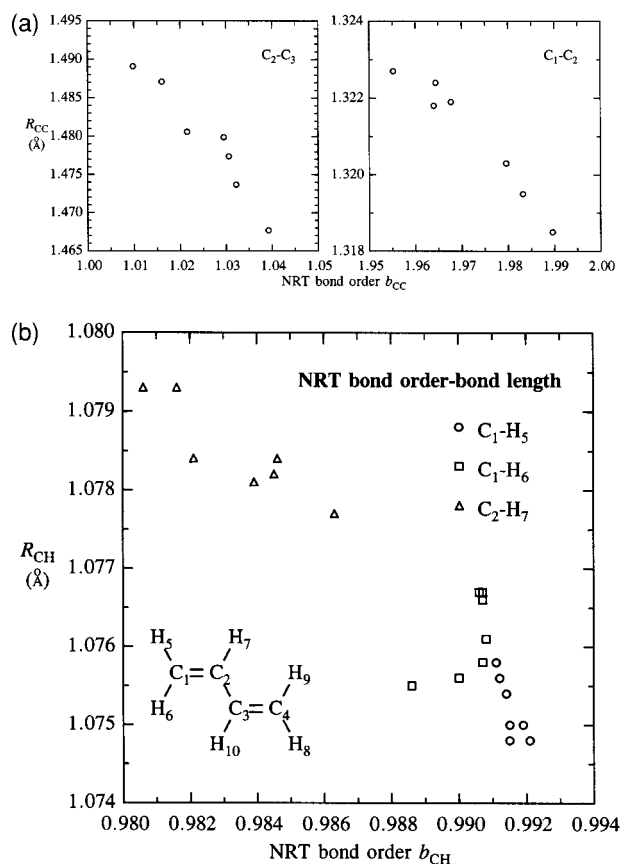agree with these predictions. Figure 2b displays the plot of NRT bond order (idealized) vs. CH

FIGURE 2. (a) Correlation of NRT bond order (idealized PG geometry) with CC bond lengths (optimized RHF / 6-31G*) for central C_2—C_3 bond (left) and terminal C_1=C_2 bond (right) of twisted butadienes (cf. Fig. 1). (b) Similar to (a), for C_1—H_5 (circles), C_1—H_6 (squares), and C_2—H_7 (triangles).

cess, we considered synchronous conrotatory or disrotatory dihedral rotations of rigid trigonal methylene groups (all other variables retaining fixed Pople-Gordon values) at the RHF/6-31G* level. As expected, the conrotatory pathway leads to more pronounced bond rearrangements; for example, near $\phi = 110°$, the weight of cyclobutene-like resonance structures is about twice as large in the conrotatory as in the disrotatory form (20.7% vs. 10.4%). The variations of NRT bond order (default program settings; Fig. 3, solid lines) along the conrotatory pathway are shown in Figure 3. One can recognize the characteristic butadiene-like pattern (at left) and cyclobutene pattern (at right), separated by a "transition region" (near 104°) where a two-reference optimization is performed. Because the default "boundary" between secondary reference is an arbitrary program threshold ($w_{ref} \geq 0.35^* w_{max}$), passage through the transition region necessarily results in discontinuities at these boundaries. This example emphasizes the need to select and impose (with the $NRTSTR keylist) a common set of reference structures to traverse a desired transition region. To illustrate this option, Figure 3 also shows the alternative two-reference bond orders (dashed lines) that result when buta-

bond length (optimized) for all points along the torsional coordinate, showing that there is a modest but significant correlation between quantitative NRT values and small geometry variations even at this greatly expanded scale.

We can also use this example to illustrate further the type of "discontinuity" that occurs when the default NRT program encounters a change in the number or type of reference structures. For this purpose, we consider the model ring closure that results when the two terminal methylene groups of *cis*-butadiene are twisted face-to-face to form cyclobutene, breaking $\pi_{C_1-C_2}$, $\pi_{C_3-C_4}$ to form new $\sigma_{C_1-C_4}$, $\pi_{C_2-C_3}$ bonds. According to the well-known Woodward-Hoffman rules, simultaneous dihedral twists ϕ_{12}, ϕ_{34} can be carried out in a conrotatory ($\phi_{12} = \phi_{34}$) or disrotatory ($\phi_{12} = -\phi_{34}$) sense, the former leading to "allowed" bond rearrangements. As a simple model of such a pro-
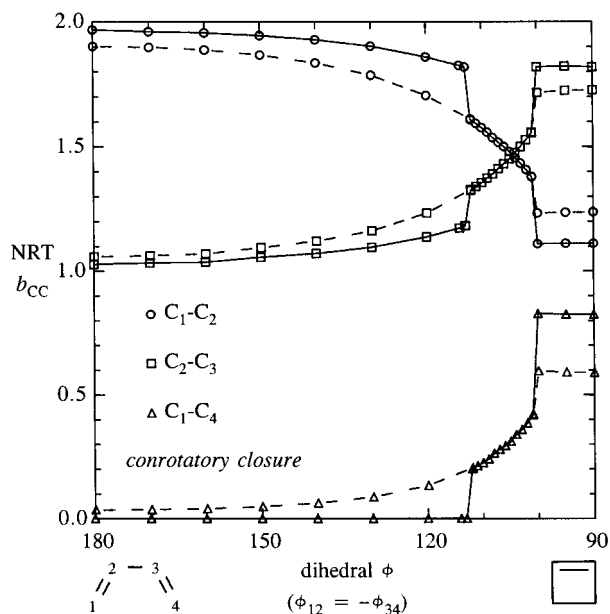

FIGURE 3. Variations of NRT b_{CC} bond orders b_{12} (circles), b_{23} (squares), and b_{14} (triangles), for idealized butadiene → cyclobutene isomerization by conrotatory ring closure (RHF / 6-31G* level), showing differences between default NRT treatment (solid lines) and uniform two-reference treatment (dashed lines) specified with the $NRTSTR keylist.

diene and cyclobutene are both treated as reference structures at all angles, avoiding the "discontinuity" (near 112°) of the default treatment. (The remaining discontinuity near 100° reflects an abrupt change in the character of the MO wave function, not an NRT threshold artifact.) This example emphasizes again that valid NRT comparisons of distinct regions of the potential energy surface should be based on a consistent choice of common reference structures.

POLAR COVALENCY AND ELECTROVALENCY: FLUOROMETHANES

To test the NRT description of atomic valency in polar and nonpolar compounds, we considered the family of fluoromethanes, CH_nF_{4-n}, $n = 1-4$. This allows us to investigate the NRT covalency (C_X), electrocovalency (E_X), and total valency (V_X) of $X = C, F, H$ atoms in molecules of varying polarity, for comparison with expected empirical values.

Figures 4a–c illustrates the calculated NRT values of C_X (triangles), E_X (squares), and V_X (circles) for carbon (Fig 4a), hydrogen (Fig. 4b), and fluorine (Fig. 4c) atoms in the fluoromethane series, described at the RHF/6-31G* level (idealized PG geometry). As is shown in this figure, the NRT covalency and electrovalency vary in a chemically reasonable way, with the electrovalency increasing as the polar character of attached bonds increases. Thus, the NRT covalency of carbon decreases from 3.1317 (in CH_4) to 1.9495 (in CF_4), while the electrovalency correspondingly increases. Despite these variations, the *total* NRT valency is seen to be remarkably constant throughout the series ($V_C = 3.99 \pm 0.01$, $V_H = 0.99 \pm 0.01$, $V_F = 1.00 \pm 0.02$), in excellent agreement with the expected empirical (tetra- or uni-) valency. Thus, Figure 4a–c illustrates the *complementary* character of electrovalent and covalent contributions to total atomic valency and indicates why bond indices that neglect one or the other aspect may fail to give consistent agreement with experimentally observed valency values.

We also calculated C—F bond orders at the higher RHF/6-311 + + G** level (PG geometry[31]) in order to make comparisons with available CM values for this series.[20, 22] Results are shown in Table VII, where we also include comparisons with corresponding WBI and MM values. The NRT results suggest the expected C—F single bonds throughout the series ($b_{CF} = 1.01 \pm 0.01$), and the

WBI and MM values (0.85 ± 0.02, 0.95 ± 0.09, respectively) are crudely in agreement. But the CM values vary in the range 0.54–0.75 (with a trend *opposite* that of the WBI and MM indices) as fluorine ligancy is varied. The CM value crudely approximates the NRT covalency for CF_4 (0.543 vs. 0.531), but these values become widely discrepant (and trend in opposite directions) as fluorines are removed. A particularly discrepant feature of the CM bond indices (not apparent from the results of Wiberg and Rablen[22] but explicity indicated by Ciowlowki and Mixon[20] for CHF_3) is the surprisingly large F—F bond order (0.171, nearly one-third as large as the C—F bond order), which has no counterpart in the WBI (0.03), MM (0.01), or NRT (0.00) descriptions.

Similar conclusions can be drawn from atomic valency values (not tabulated), where the NRT results give fairly "ordinary" values for carbon (3.992 ± 0.003), hydrogen (0.985 ± 0.007), and fluorine (1.01 ± 0.01) throughout the series. The alternative MO-based valencies are much less orderly; for example, at the RHF/6-311 + + G** level, the values of V_C vary in the range 3.49–3.73 for the Wiberg index and 3.83–4.18 for the MM index (with opposite trends as fluorine ligancy is varied). For the CM method, tabulated[20] orders for CHF_3 allow one to infer fairly reasonable values for fluorine and hydrogen ($V_F = 0.979$, $V_H = 1.062$), but an unreasonably low value for carbon ($V_C = 2.583$),[32] well outside the range of other indices. These results seem to confirm the general superiority of the NRT description for polar covalent compounds and raise questions concerning the premises of the CM treatment.

OPEN SHELL SPECIES: HYDROXYMETHYL RADICAL

Finally, to demonstrate the application of NRT analysis to an open-shell species, we consider the hydroxymethyl radical (CH_2OH) as described at UHF/6-31G* (uncorrelated) and UMP2/6-31G* (correlated) levels of theory. Because this species is known to have "floppy" geometry, we optimized the radical structure at each level (C_s symmetry: see Table VIII) before performing NRT analysis.

Consistent with the "different Lewis structures for different spins" open-shell NBO picture that was previously applied to such species,[33] the NRT procedure is applied separately to density matrices for alpha and beta spin. This leads to the NRT weightings shown in Table IX, which exhibits the
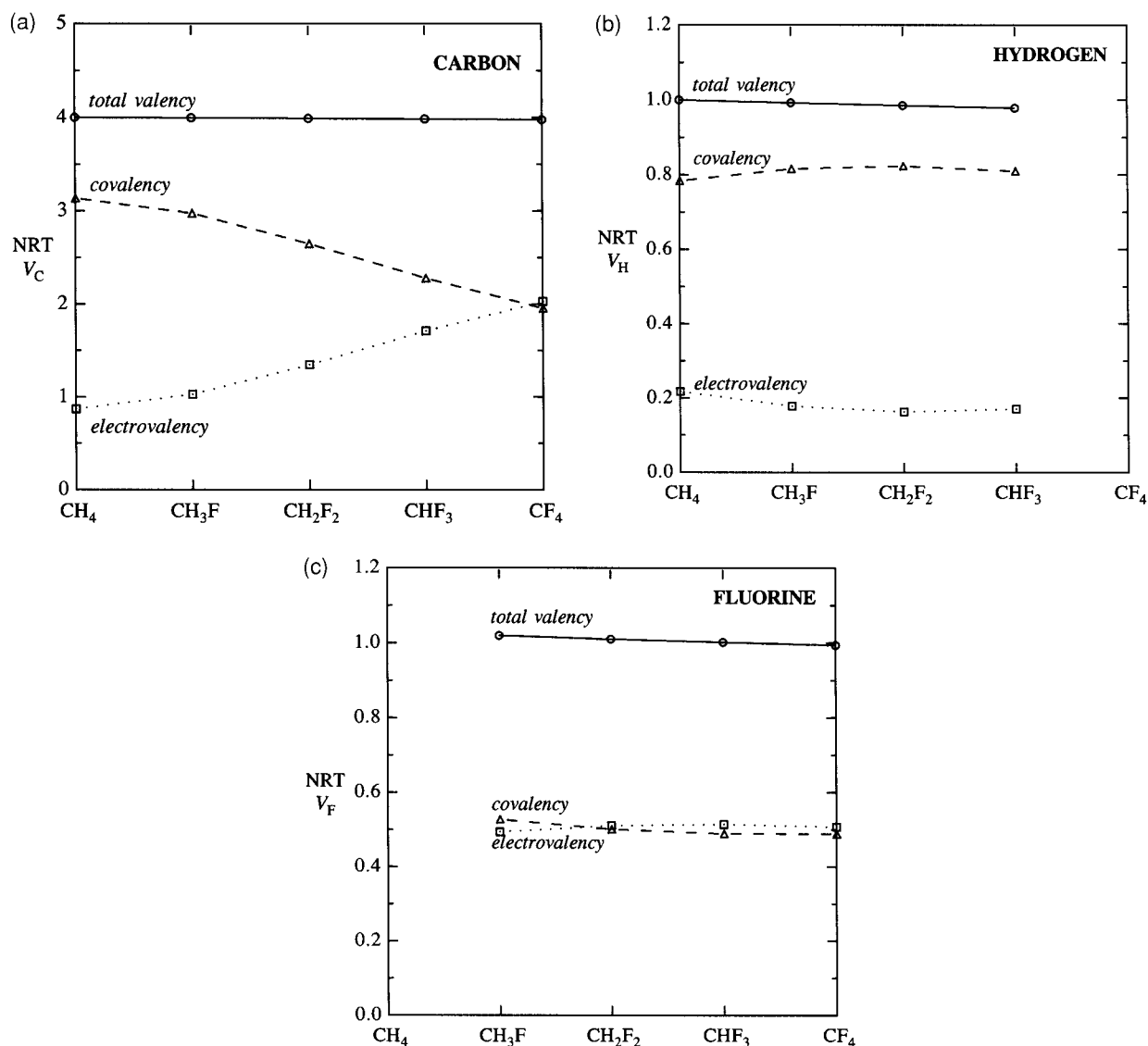
FIGURE 4. (a) Variations of carbon atom electrovalency (squares), covalency (triangles), and total valency (circles) in the fluoromethanes, CF_nH_{4-n}, calculated at RHF / 6-31G* level (idealized Pople-Gordon geometry), showing "complementary" electrovalent and covalent contributions to total atomic valency. (b) Similar to (a), for hydrogen atom. (c) Similar to (a), for fluorine atom.

separate weightings $(w_i^{(\alpha)}, w_i^{(\beta)})$ for each structure i in the two spin sets. As a notational device to avoid explicit depiction of all nonbonded "lone" electrons, we have included "formal charge" labels to indicate how many nonbonded electrons must be added or subtracted to obtain the full Lewis structure specification. For example, the leading alpha structure in Table IX has one lone α electron on carbon (to give formal charge of -1) and two on oxygen (the usual electroneutral pattern), to give the overall -1 formal charge of the "anion-like" alpha spin set, whereas, the corre-

sponding "cation-like" beta structure has no lone β electrons on C (formal charge $+1$) but the usual two on O. (Of course, the "formal charges" have but loose connection to the physical charge distribution as described, e.g., by natural population analysis.) Note that, in the NRT framework, a "resonance structure" is simply a pattern of one-center (nonbonded) and two-center (bonded) spin orbitals occupied by electrons of the given spin, and there is no intrinsic reason why these structures should be identical for α and β spins. Indeed, because the open-shell spatial distributions

TABLE VII.

Calculated C—F and C—H Bond Orders for Fluoromethanes at RHF / 6-311 + + G** Level (PG Geometry Except for CM Values: See Reference 31), Showing the Comparison between NRT, Wiberg (WBI), Mayer-Mulliken (MM), and Cioslowski-Mixon (CM) Values.

Bond	NRT bond order			Other		
	Total	Covalent	Ionic	WBI	MM	CM
C—F bond						
CF_4	0.9976	0.5314	0.4663	0.8727	1.0443	0.543
CHF_3	1.0038	0.5221	0.4817	0.8534	1.0052	0.616
						(0.572)[a]
CH_2F_2	1.1019	0.5204	0.4906	0.8391	0.9523	0.688
CH_3F	1.0193	0.5284	0.4909	0.8295	0.8579	0.747
C—H bond						
CHF_3	0.9785	0.8611	0.1174	0.9474	0.9921	(0.867)[a]
CH_2F_2	0.9844	0.8686	0.1158	0.9580	0.9988	
CH_3F	0.9920	0.8555	0.1365	0.9661	0.9913	

[a] RHF / 6-31 + + G** values.[20]

of α and β electrons are different, the optimal NRT representations of α and β distribution are expected to be unequivalent, as Table IX shows to be the case.

It is apparent from Table IX that β (minority spin) electrons are significantly more delocalized than α (majority spins) electrons. This is chemically reasonable; since the β system has a vacancy on carbon that interacts strongly with nonbonded electrons of the adjacent oxygen atom to give the formal "dative pi bond" of structure 2.β. The stronger β resonance delocalization is also manifested in significantly higher CO bond order in the β system (viz. 0.55 vs. 0.53 at UMP2 level) as well as higher CO polarity (45% vs. 40% ionic character). Table X shows that the percentage ionicity tends to be systematically higher in correlated wave functions and to be noticeably increased by resonance delocalization.

The atomic valency of carbon is seen to be significantly altered from its normal closed-shell value, consistent with the NRT resonance struc-

tures. For example, in the α set, carbon resembles a nitrogen atom (with filled nonbonding orbital; cf. $\ddot{N}H_2OH$) whereas, in the β set, it resembles boron (with empty p-type orbital), both nominally "trivalent" ($V_C = 3.05$ at the correlated level). However, the corresponding valencies of hydrogen (0.98) and oxygen (2.05) are affected little by the radical delocalization. The tabulated valencies thus seem to reflect well the chemical behavior at each atom.

Conclusions

We have introduced formal definitions of "natural bond order" and "natural atomic valency" in the framework of natural resonance theory (NRT) and illustrated the *ab initio* application of these formulas to several prototype cases involving weak or moderate resonance delocalization. These applications serve to document the convergence, stabil-

TABLE VIII.

Optimized Bond Lengths R (Å) and Valence and Dihedral Angles θ, ϕ (in Degrees) for Hydroxymethyl Radical (C_S-Symmetry) at Uncorrelated (UHF / 6-31G*) and Correlated (UMP2 / 6-31G*) Levels.

Level	R_{CO}	R_{OH}	R_{CH}	θ_{COH}	θ_{OCH}	ϕ_{HOCH}
UHF / 6-31G*	1.3625	0.9496	1.0758	111.1641	118.0999	79.9701
UMP2 / 6-31G*	1.3821	0.9715	1.0849	109.1036	116.5910	104.9062

[a] Note that the (slight) pyramidalization of the methylene group is of opposite sense in the two levels.

TABLE IX.
Leading NRT Resonance Weights (α and β Spin) for Hydroxymethyl Radical at Uncorrelated MO (UHF / 6-31G*) and Correlated (UMP / 6-31G*) Levels of Theory (Nonbonded Electrons Are Suppressed in the Lewis Structure Representations).[c]

i	Alpha structure	$w_i^{(\alpha)}$ (%, α spin) MO[a]	$w_i^{(\alpha)}$ (%, α spin) corr[b]	Beta structure	$w_i^{(\beta)}$ (%, β spin) MO[a]	$w_i^{(\beta)}$ (%, β spin) corr[b]
1.	H₂C⁻—O—H	[97.20]	[95.39]	H₂C⁺—O—H	[93.91]	[89.28]
2.	H₂C=O ... H⁻	1.03	1.52	H₂C=O⁺—H	2.80	4.65
3.	H₂C⁻=O⁺—H, H⁻	0.77 (2)	1.55 (2)	H₂C⁺=O⁺—H, H⁻	0.78 (2)	1.55 (2)
4.	H₂C⁻ ... O⁻—H, H⁺	0.11 (2)	< 0.01	H₂C=O ... H⁺	1.72	2.98

[a] UHF / 6-31G*.
[b] UMP2 / 6-31G*.
[c] Brackets identify reference structures; parenthesized numbers give degeneracy factors for equivalent structure formulas.

ity with respect to basis set extension, dependence on program parameters, and general practicality of the NRT method for typical open- and closed-shell species at both uncorrelated and correlated levels of theory. Our results also demonstrate the higher level of quantitative detail and the improved correlations of bond order and valency indices with empirical structural and chemical properties that are achieved by the NRT expansion.

Although the underlying formulation of NRT differs substantially from that of Pauling-Wheland theory, the new method retains a strong associa-tion with the classical resonance concepts. The high percentage of delocalization density recovered by the NRT expansion (typically 80–90%, with relatively small numbers of resonance structures) seems to attest to the validity and accuracy of resonance-theoretic assumptions that underlie many concepts of physical organic chemistry.

Compared to previous methods for calculating resonance weightings, bond order, and atomic valency, the NRT approach offers several important advantages. 1) The NRT statistical weighting distribution is derived from a *variational criterion*,

TABLE X.
Open-Shell α and β NRT Bond Orders b_{AB} and Atomic Valencies V_A (with Percentage Ionicity in Parentheses) for Hydroxymethyl Radical, Calculated at Uncorrelated MO (UHF / 6-31G*) and Correlated (UMP2 / 6-31G*) Levels (cf. Table IX).

	MO(UHF / 6-31G*) α	MO(UHF / 6-31G*) β	MO(UHF / 6-31G*) Total	corr(UMP2 / 6-31G*) α	corr(UMP2 / 6-31G*) β	corr(UMP2 / 6-31G*) Total
b_{CO}	0.5117 (37%)	0.5304 (45%)	1.0422	0.5230 (40%)	0.5536 (45%)	1.0767
b_{OH}	0.4948 (47%)	0.4914 (52%)	0.9862	0.4924 (57%)	0.4851 (52%)	0.9775
b_{CH}	0.4956 (20%)	0.4961 (9%)	0.9917	0.4923 (20%)	0.4923 (13%)	0.9845
V_C	1.5029 (26%)	1.5226 (22%)	3.0255	1.5076 (27%)	1.5382 (24%)	3.0458
V_O	1.0066 (42%)	1.0219 (48%)	2.0284	1.0155 (44%)	1.0387 (48%)	2.0542

based on minimizing the "error" δ_W of the description. Thus, the NRT parameters are derived purely from theory, and the accuracy of the NRT description can be assessed *internally* from the optimal δ_W value, without appeal to external empirical data. 2) Electrovalent and covalent contributions to bond order are treated in a unified manner (specifically avoiding the Pauling-Wheland "covalent-ionic resonance" concept). Thus, the NRT description is uniformly applicable to a wide variety of organic and inorganic species, permitting consistent comparisons among diverse systems. 3) NRT analysis can be readily integrated into popular electronic structure packages for routine application to wave functions produced by state-of-the-art *ab initio* methods (including SCF, MCSCF, CI, and Møller-Plesset perturbative treatments). Thus, the NRT method may be used to bring resonance theory concepts back into the mainstream of *ab initio* studies.

Although the present paper has focused on documenting the performance of the NRT method for typical saturated and unsaturated species, the method is readily applicable to a much broader variety of exceptional or "anomalous" bonding types. Examples of such applications are presented in the following paper.

Acknowledgments

References

1. (a) L. Pauling and G. W. Wheland, *J. Chem Phys.*, **1**, 362 (1933); G. W. Wheland and L. Pauling, *J. Am. Chem. Soc.*, **57** 2086, (1935), G. W. Wheland, *The Theory of Resonance and Its Application to Organic Chemistry*, John Wiley, New York, 1955. (b) L. Pauling, *Nature of the Chemical Bond*, 3rd ed., Cornell University Press, Ithaca, NY, 1960.

2. P.-O Löwdin, *Phys. Rev.*, **97**, 1474, (1955); E. R. Davidson, *Density Matrices in Quantum Chemistry*, Academic, New York, 1976.

3. J. P. Foster and F. Weinhold, *J. Am. Chem. Soc.*, **102**, 7211 (1980); A. E. Reed and F. Weinhold, *J. Chem. Phys.*, **78**, 4066 (1983); A. E. Reed, R. B. Weinstock, and F. Weinhold, *J. Chem. Phys.*, **83**, 735 (1985); A. E. Reed and F. Weinhold, *J. Chem. Phys.*, **83**, 1736 (1985).

4. NBO Program: E. D. Glendening, A. E. Reed, J. E. Carpenter, and F. Weinhold, *QCPE Bull.*, **10**, 58 (1990); A. E. Reed and F. Weinhold *QCPE Bull.*, **5**, 141 (1985). Reviews of NBO Method and Applications: A. E. Reed, L. A. Curtiss, and F. Weinhold, *Chem. Rev.*, **88**, 899 (1988); F. Weinhold and J. E. Carpenter, in R. Naaman and Z. Vager (eds.), *The Structure of Small Molecules and Ions*, Plenum, New York, 1988.

5. (a) Bond length: L. Pauling, *J. Am. Chem. Soc.*, **69**, 542 (1947); Reference 1(b), p. 255; C. A. Coulson, *Proc. R. Soc. London*, **A207**, 91 (1951); C. A. Coulson and A. Golebiewski, *Proc. Phys. Soc.*, **78**, 1310 (1961); G. Grampp, M. Cebe, and E. Cebe, *Z. Phys. Chem.*, **166**, 93 (1990). (b) Bond energy: H. S. Johnson, *Adv. Chem. Phys.*, **3**, 131 (1960); H. S. Johnston and A. C. Parr, *J. Am. Chem. Soc.*, **85**, 2544 (1963); N. Agmon and R. D. Levine, *J. Chem. Phys.*, **71**, 3034 (1979); P. Politzer and S. Ranganathan, *Chem. Phys. Lett.*, **124**, 527 (1986). (c) Other: W. Gordy, *J. Chem. Phys.*, **14**, 305 (1946); L. Peter, *J. Chem. Ed.*, **63**, 123 (1986); M. Barfield, M. J. Collins, J. E. Gready, S. Sternhell, and C. W. Tansey, *J. Am. Chem. Soc.*, **111**, 4285 (1989); D. K. Maity and S. P. Bhattacharyya, *J. Am. Chem. Soc.*, **112**, 3223 (1990).

6. L. Pauling, L. O. Brockway, and J. Y. Beach, *J. Am. Chem. Soc.*, **57**, 2705 (1935).

7. Reference 1(b), p. 282.

8. Reference 1(b), p. 499; Pauling, L. *Proc. Roy. Soc. London*, **A356**, 433 (1977).

9. Useful discussion of the nature of valency, electrovalency, and covalency from a historical perspective are given by N. V. Sidgwick, *The Electronic Theory of Valency*, Oxford University Press, Longon, 1929, particularly Chapter VI; C. A. Russell, *History of Valency*, University Press, Leicester, 1971.

10. In principle, one might have (e.g., for an excited state) higher occupancy of an antibond than of the corresponding bond, which would lead to a net negative contribution to formal bond order. However, this situation is not provided for in the present version of the NRT program.

11. See, e.g., Reference 1(b) pp. 88–95, for discussion of the relationship of bond energies to electronegativity differences.

12. C. A. Coulson, *Proc. R. Soc. London*, **A169**, 413 (1939), **A207**, 91 (1951); C. A. Coulson, *Valence*, 2nd ed., Oxford University Press, London, 1961, pp. 266–270.

13. K. B. Wiberg, *Tetrahedron*, **24**, 1083 (1968).

14. D. R. Armstrong, P. G. Perkins, and J. J. P. Stewart, *J. Chem Soc.*, *Dalton Trans.*, **1973**, 838 (1973); N. P. Boresova and S. G. Semenov, *Vestn. Leningrad Univ.*, **16**, 119 (1973); M. S. Gopinathan and K. Jug, *Theor. Chim. Acta*, **63**, 497, 511 (1983); I. Mayer and M. Revesz, *Inorg. Chim. Acta*, **77**, L205 (1983); I. Mayer, *Chem. Phys. Lett.*, **97**, 270 (1983); I. Mayer, *Int. J. Quantum Chem.*, **26**, 151 (1984); M. S. de Giambiagi, M. Giambiagi, and F. E. Jorge, *Z. Naturforsch.*, **A39**, 1259 (1984); M. A. Natiello and J. A. Medrano, *Chem. Phys. Lett.*, **105**, 180 (1984); K. Jug, *J. Comput. Chem.*, **5**, 555 (1984); I. Mayer, *Int. J. Quantum Chem.*, **29**, 477 (1986); I. Mayer, *J. Mol. Struct. Theochem.*, **149**, 81 (1957); K. Jug, E. Fasold, and M. S. Gopinathan, *J. Comput. Chem.*, **10**, 965 (1989); G. Lendvay, *J. Phys. Chem.*, **93**, 4422 (1989).

15. For critical discussion of the terminology employed by Jug and coworkers,[14] see I. Mayer, *Theor. Chim. Acta*, **67**, 315 (1985); note that the orbitals called "natural hybrid orbitals" and "natural bond orbitals" by Jug and coworkers in 1983

are unrelated to the corresponding quantities defined previously in references 3 and 4.

16. The quantities introduced by I. Mayer[14] are closely associated with Mulliken population analysis and its well-known pathologies in larger basis sets. For example, Baker [J. Baker, *Theor. Chim. Acta*, **68**, 221 (1985)] cites an example in which the calculated Mayer valency of carbon changes from $+3.39$ to $-(!)4.86$ when diffuse functions are added.

17. Jug and coworkers (see citations in reference 14) have variously suggested Wiberg's formula with no overlap, with Löwdin orthogonalization, and with a modified scheme of occupancy-weighted symmetric orthogonalization.

18. F. Weinhold and J. E. Carpenter, *J. Mol. Struct. Theochem.*, **165**, 189 (1980).

19. A. E. Reed and P. v. R. Schleyer, *Inorg Chem.*, **27**, 3969 (1988); *J. Am. Chem. Soc.*, **112**, 1434 (1990).

20. J. Cioslowski and S. T. Mixon, *J. Am. Chem. Soc.*, **113**, 4142 (1991).

21. R. F. W. Bader and T. T. Nguyen-Dang, *Adv. Quantum Chem.*, **14**, 63 (1981).

22. K. B. Wiberg and P. R. Rablen, *J. Am. Chem. Soc.*, **115**, 614 (1943).

23. I. D. Brown and R. D. Shannon, *Acta Crystall.*, **A29**, 266 (1973); I. D. Brown and D. Altermatt, *Acta Crystall.*, **B41**, 244 (1985). For applications, see I. D. Brown, *J. Solid State Chem.*, **82**, 122 (1989); M.-H. Whangbo and C. C. Torardi, *Science*, **249**, 1143 (1990).

24. W. G. Penny, *Proc. R. Soc. London*, **A158**, 306 (1937); W. C. Herndon, *J. Am. Chem. Soc.*, **95**, 2404 (1973); I. Gutman and N. Trinajstic, *Top. Curr. Chem.*, **42**, 49 (1973); I. Gutman and H. Sachs, *Z. Phys. Chem.*, **268**, 257 (1987), and references therein.

25. J. A. Pople and M. Gordon, *J. Am. Chem. Soc.*, **87**, 4253 (1967).

26. For a comprehensive description of computational methods and basis set designations used herein, see W. J. Hehre, L. Radom, P. v. R. Schleyer, and J. A Pople, *Ab Initio Molecular Orbital Theory*, John Wiley, New York, 1986. All wave function calculations were performed with the Gaussian 92 program system: M. J. Frisch, G. W. Trucks, M. Head-Gordon, P. M. W. Gill, M. W. Wong, J. B. Foresman, B. G. Johnson, H. B. Schlegel, M. A. Robb, E. S. Repogle, R. Gomperts, J. L. Andres, K. Raghavachari, J. S. Binkley, C. Gonzalez, R. L. Martin, D. J. Fox, D. J. Defrees, J. Baker, J. J. P. Stewart, and J. A. Pople, *Gaussian 92, Revision A*, Gaussian, Inc., Pittsburgh, 1992.

27. Note that bond order–bond length correlations are not necessarily expected to be linear. For example, Coulson[12] originally suggested a linear relation between bond length and P_{AB}, but the same cannot be expected for MM, WBI, and Jug indices, which are quadratic in P_{AB}.

28. Of course, it is quite artificial to consider such a ''transition'' in the present case; the default NRTWGT criterion for acceptance as a reference structure ($w_\alpha \geq 0.35 * w_{max}$) ensures that only the most strongly delocalized systems will have more than a single reference structure.

29. The default NRT expansions for these wave functions include about 20 additional structures (not shown) with smaller weightings $\geq 0.01\%$.

30. The superficially high weight of ''long bond'' structures in earlier RT treatments can be attributed to the ''overcorrelation'' artifact of Heitler-London valence-bond wave functions; see R. McWeeny, *Proc. R. Soc. London*, **A223**, 63, 306 (1954).

31. This differs slightly from the geometries employed by Cioslowki and Mixon[20] (optimized HF/6-31G*) and Wiberg and Rablen[22] (partially optimized MP2/6-31G*, with C-F bonds constrained to equal the value for CH_3F). These geometry differences are likely to be unimportant on the scale of the comparisons considered here. The large difference between CHF_3 values of b_{CF} reported in references 20 (0.572, RHF/6-31++G** level) and 22 (0.616 RHF/6-311 ++G** level) is therefore puzzling.

32. The CM V_C is rather close to the NRT covalency (2.427) in this case, but the corresponding valencies for fluorine differ by almost a factor of two.

33. J. E. Carpeter and F. Weinhold, *J. Mol. Struct. Theochem.*, **169**, 41 (1988).